

See discussions, stats, and author profiles for this publication at: <https://www.researchgate.net/publication/260912988>

# Influence of Substituent Effects on the Formation of (PCI)-C-... Pnicogen Bonds or Halogen Bonds

ARTICLE in THE JOURNAL OF PHYSICAL CHEMISTRY A · MARCH 2014

Impact Factor: 2.69 · DOI: 10.1021/jp500915c · Source: PubMed

---

CITATIONS

18

---

READS

29

3 AUTHORS, INCLUDING:



Ibon Alkorta

Spanish National Research Council

680 PUBLICATIONS 12,430 CITATIONS

SEE PROFILE



José Elguero

Spanish National Research Council

1,502 PUBLICATIONS 22,206 CITATIONS

SEE PROFILE

## Influence of Substituent Effects on the Formation of P...Cl Pnictogen Bonds or Halogen Bonds

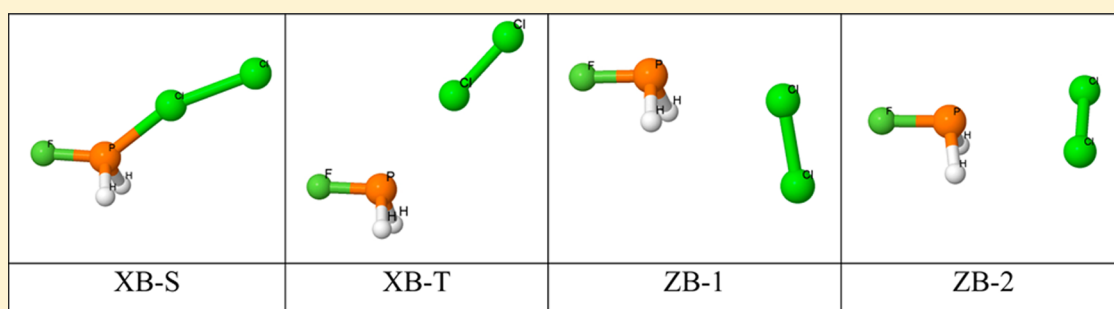
Janet E. Del Bene\*

Department of Chemistry, Youngstown State University, Youngstown, Ohio 44555, United States

Ibon Alkorta\* and José Elguero

Instituto de Química Médica (IQM-CSIC), Juan de la Cierva, 3, E-28006 Madrid, Spain

## S Supporting Information



**ABSTRACT:** Ab initio MP2/aug'-cc-pVTZ calculations have been carried out in search of equilibrium structures with P...Cl pnictogen bonds or halogen bonds on the potential energy surfaces  $\text{H}_2\text{FP}:\text{ClY}$  for  $\text{Y} = \text{F}, \text{NC}, \text{Cl}, \text{CN}, \text{CCH}, \text{CH}_3$ , and  $\text{H}$ . Three different types of halogen-bonded complexes with traditional, chlorine-shared, and ion-pair bonds have been identified. Two different pnictogen-bonded complexes have also been found on these surfaces. The most electronegative substituents  $\text{F}$  and  $\text{NC}$  form only halogen-bonded complexes, while the most electropositive substituents  $\text{CH}_3$  and  $\text{H}$  form only pnictogen-bonded complexes. The halogen-bonded complexes involving the less electronegative groups  $\text{Cl}$  and  $\text{CN}$  are more stable than the corresponding pnictogen-bonded complexes, while the pnictogen-bonded complexes with  $\text{CCH}$  are more stable than the corresponding halogen-bonded complex. Traditional halogen-bonded complexes are stabilized by charge transfer from the  $\text{P}$  lone pair to the  $\text{Cl}-\text{A} \sigma^*$  orbital, where  $\text{A}$  is the atom of  $\text{Y}$  directly bonded to  $\text{Cl}$ . Charge transfer from the  $\text{Cl}$  lone pair to the  $\text{P}-\text{F} \sigma^*$  orbital stabilizes pnictogen-bonded complexes. As a result, the  $\text{H}_2\text{FP}$  unit becomes positively charged in halogen-bonded complexes and negatively charged in pnictogen-bonded complexes. Spin-spin coupling constants  $^{1X}\text{J}(\text{P}-\text{Cl})$  for complexes with traditional halogen bonds increase with decreasing  $\text{P}-\text{Cl}$  distance, reach a maximum value for complexes with chlorine-shared halogen bonds, and then decrease and change sign when the bond is an ion-pair bond.  $^{1\text{P}}\text{J}(\text{P}-\text{Cl})$  coupling constants across pnictogen bonds tend to increase with decreasing  $\text{P}-\text{Cl}$  distance.

## ■ INTRODUCTION

Noncovalent interactions play a very important role in supramolecular chemistry, molecular biology, and materials science. Traditionally, research in this field has focused on the most common and well-known noncovalent interaction, the hydrogen bond. However, in the last few decades, interest in the halogen bond<sup>1–3</sup> and more recently, the pnictogen bond<sup>4–7</sup> has increased significantly. Halogen bonds and pnictogen bonds arise when a halogen atom or a pnictogen atom acts as the Lewis acid in a Lewis acid–Lewis base intermolecular interaction.

The molecules involved in the formation of halogen bonds and pnictogen bonds usually have molecular electrostatic potentials (MEPs) at a particular atom in the molecule which exhibit both positive regions or  $\sigma$ -holes<sup>8</sup> and negative regions corresponding to lone pairs or  $\pi$  electrons, as illustrated in Figure 1. If two such molecules interact, then in principle they

should be able to form either halogen-bonded or pnictogen-bonded complexes, depending on which molecule is the electron-pair donor and which is the acceptor. Literature describing both kinds of bonds is abundant, and some recent papers have compared these two types of intermolecular interactions.<sup>9–12</sup> However, to our knowledge, the present paper is the first study in which the same monomers compete to form a halogen bond (XB) or a pnictogen bond (ZB). Could substituent effects be used to preferentially select the type of bond formed?

To answer this question, we have investigated a series of complexes involving  $\text{H}_2\text{FP}$  and molecules  $\text{ClY}$ , with the

Received: January 26, 2014

Revised: March 4, 2014

Published: March 19, 2014

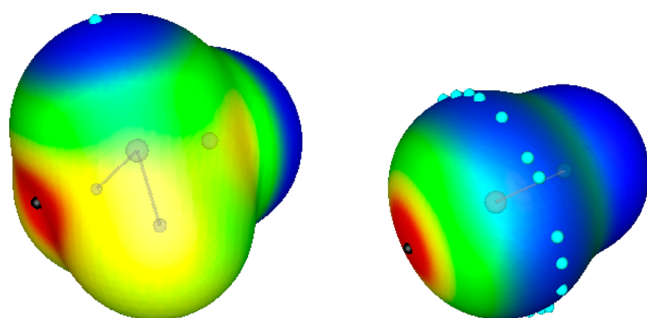


**Figure 1.** MEPs of  $\text{H}_2\text{FP}$  and  $\text{ClY}$ . Black dots indicate the position of the  $\sigma$ -holes while light blue dots are associated with the lone pairs.

substituents  $\text{Y} = \text{F}, \text{NC}, \text{Cl}, \text{CN}, \text{CCH}, \text{CH}_3$ , and  $\text{H}$ . Because both  $\text{P}$  and  $\text{Cl}$  have  $\sigma$ -holes and lone pairs, in principle two types of complexes could be formed, one stabilized by a  $\text{P}\cdots\text{Cl}$  halogen bond, and the other by a  $\text{P}\cdots\text{Cl}$  pnictogen bond. We have examined the  $\text{H}_2\text{FP}:\text{ClY}$  potential surfaces in search of these complexes. In this paper we describe the equilibrium halogen-bonded and pnictogen-bonded complexes found on these surfaces and note what circumstances favor one bond over the other. We then present the structures and binding energies of these complexes, their bonding properties, and the one-bond NMR spin–spin coupling constants  $^{1X}\text{J}(\text{P}–\text{Cl})$  and  $^{1P}\text{J}(\text{P}–\text{Cl})$  across halogen and pnictogen bonds, respectively.

## METHODS

The structures of the isolated monomers and complexes were optimized at second-order Møller–Plesset perturbation theory (MP2)<sup>13–16</sup> with the aug'-cc-pVTZ basis set.<sup>17</sup> This basis set is derived from the Dunning aug-cc-pVTZ basis set<sup>18,19</sup> by removing diffuse functions from H atoms. Frequencies were computed to establish that the optimized structures correspond to equilibrium structures on their potential surfaces. Optimization and frequency calculations were performed using the Gaussian 09 program.<sup>20</sup>

The electron densities of the complexes have been analyzed using the atoms in molecules (AIM) methodology<sup>21–24</sup> employing the AIMAll program.<sup>25</sup> The topological analysis of the electron density produces the molecular graph of each complex. This graph identifies the location of electron density features of interest, including the electron density ( $\rho$ ) maxima associated with the various nuclei, saddle points which correspond to bond critical points (BCPs), and ring critical points which indicate a minimum electron density within a ring. The zero gradient line which connects a BCP with two nuclei is the bond path. Natural bond order (NBO)<sup>26</sup> MP2/aug'-cc-pVTZ electron populations have been evaluated for monomers and complexes. In addition, the NBO method has also been used to analyze the stabilizing charge-transfer interactions using the NBO-6 program.<sup>27</sup> NBO orbitals have been represented with the Jmol program<sup>28</sup> using the tools developed by Marcel Patek.<sup>29</sup>

Spin–spin coupling constants were evaluated using the equation-of-motion coupled cluster singles and doubles (EOM-CCSD) method in the CI (configuration interaction)-like approximation,<sup>30,31</sup> with all electrons correlated. For these calculations, the Ahlrichs qzp basis set<sup>32</sup> was placed on  $^{13}\text{C}$ ,  $^{15}\text{N}$ , and  $^{19}\text{F}$ , and the qz2p basis set on  $^{31}\text{P}$  and  $^{35}\text{Cl}$ . The Dunning cc-pVDZ basis set was placed on all  $^1\text{H}$  atoms. Only  $^{1X}\text{J}(\text{P}–\text{Cl})$  and  $^{1P}\text{J}(\text{P}–\text{Cl})$  coupling constants for halogen bonds

and pnictogen bonds, respectively, are reported in this paper. All terms which contribute to the total coupling constant, namely, the paramagnetic spin orbit (PSO), diamagnetic spin orbit (DSO), Fermi contact (FC), and spin dipole (SD), have been evaluated. The EOM-CCSD calculations were performed using ACES II<sup>33</sup> on the IBM Cluster 1350 (Glenn) at the Ohio Supercomputer Center.

## RESULTS AND DISCUSSION

Although there are many minima on the  $\text{H}_2\text{FP}:\text{ClY}$  potential surfaces, we have restricted our searches to those regions at which  $\text{P}\cdots\text{Cl}$  pnictogen-bonded and halogen-bonded complexes may exist. Three different types of halogen-bonded complexes have been found: traditional (XB-T), chlorine-shared (XB-S), and ion-pair (XB-IP), all with  $C_s$  symmetry. These are differentiated by their  $\text{P}–\text{Cl}$  and  $\text{Cl}–\text{A}$  distances, with A the atom of Y directly bonded to Cl. In addition, two types of pnictogen-bonded complexes have been identified, designated ZB-1 and ZB-2. Complexes ZB-1 have  $C_s$  symmetry with the  $\text{Cl}–\text{A}$  bond *cis* to the bisector of the  $\text{H}–\text{P}–\text{H}$  angle. Complexes ZB-2 may have either  $C_s$  or  $C_1$  symmetry, with the  $\text{Cl}–\text{A}$  bond either *trans* or *gauche*, respectively, to the bisector. These halogen- and pnictogen-bonded complexes are illustrated in Figure 2.

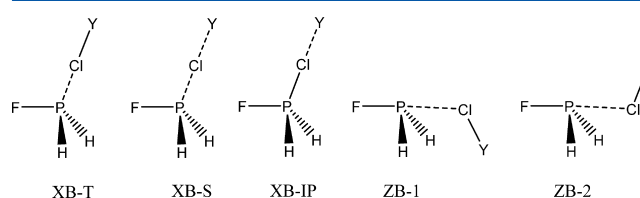


**Figure 2.** Schematic representation of the halogen-bonded and pnictogen-bonded complexes  $\text{H}_2\text{FP}:\text{ClY}$ .

The structures, total energies, and molecular graphs of halogen-bonded and pnictogen-bonded complexes are reported in Table S1 of the Supporting Information. Each graph shows a bond critical point connecting P and Cl. Table 1 presents the

**Table 1.** MP2/aug'-cc-pVTZ Binding Energies ( $\Delta E$ ,  $\text{kJ mol}^{-1}$ ) of Complexes  $\text{H}_2\text{FP}:\text{ClY}$  with Traditional (XB-T), Chlorine-Shared (XB-S), and Ion-Pair (XB-IP) Halogen Bonds and Pnictogen Bonds (ZB-1 and ZB-2)<sup>a</sup>

$\text{H}_2\text{FP}:\text{ClY}$	XB-T	XB-S	XB-IP	ZB-1	ZB-2
$\text{Y} = \text{F}$		−71.1			
NC	−13.6		−381.2 <sup>b</sup>		
Cl	−12.9	−15.3		−11.5	−10.8
CN	−8.1			−6.5	−6.3
CCH	−6.2			−11.0	−10.7
$\text{CH}_3$				−15.1	−18.3
H				−10.0	−11.6

<sup>a</sup>See Figure 1 for an identification of the types of complexes and their designations. <sup>b</sup>Binding energy relative to  $(\text{H}_2\text{FPCl})^+$  and  $\text{NC}^-$ .

binding energies of complexes  $\text{H}_2\text{FP}:\text{ClY}$  relative to the isolated monomers  $\text{H}_2\text{FP}$  and  $\text{ClY}$ , except for the ion-pair complex  $\text{H}_2\text{FPCl}^+:\text{NC}^-$ . From the data reported in Table 1, it is possible to answer the question asked in the Introduction. The preferred type of intermolecular bond can be selected by changing the nature of the substituent. When Y of ClY is a very electronegative group such as F or NC, only halogen-bonded

**Table 2.** P–Cl Distances (*R*, Å), F–P–Cl Angles ( $\angle a$ , °), and P–Cl–A Angles ( $\angle b$ , °) in Halogen-Bonded and Pnictogen-Bonded Complexes H<sub>2</sub>FP:CIY<sup>a</sup>

H <sub>2</sub> FP:CIY	XB-T			XB-S			XB-IP		
	<i>R</i>	$\angle a$	$\angle b$	<i>R</i>	$\angle a$	$\angle b$	<i>R</i>	$\angle a$	$\angle b$
Y = F				2.044	119	175			
NC	3.196	113	179				1.970	116	173
Cl	3.061	127	175	2.157	143	158			
CN	3.551	109	178						
CCH	3.542	144	163						

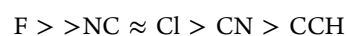
H <sub>2</sub> FP:CIY	ZB-1			ZB-2		
	<i>R</i>	$\angle a$	$\angle b$	<i>R</i>	$\angle a$	$\angle b$
Y = Cl	3.169	168	110	3.265	166	89
CN	3.365	165	95	3.437	168	81
CCH	3.295	162	93	3.320	165	85
CH <sub>3</sub>	3.157	163	100	3.121	169	90
H	3.280	167	110	3.277	169	80

<sup>a</sup>See Figure 1 for an identification of the types of complexes and their designation.

complexes are formed. This is due to the electron-withdrawing effects of these two substituents, which enhance the  $\sigma$ -hole at Cl so that it becomes a strong electron-pair acceptor for the formation of a P...Cl halogen bond and a poor electron donor for a pnictogen bond. As the electronegativity of Y decreases when the substituents are Cl, CN, and CCH, CIY becomes both an electron-pair donor in a pnictogen-bonded complex and an electron-pair acceptor in a halogen-bonded complex. The halogen-bonded complexes H<sub>2</sub>FP:ClCl and H<sub>2</sub>FP:ClCN are more stable than the corresponding pnictogen-bonded complexes, but the H<sub>2</sub>FP:ClCCH pnictogen-bonded complexes are more stable than the corresponding halogen-bonded complex. When Y is CH<sub>3</sub> or H, only complexes with pnictogen bonds are formed. These electropositive substituents essentially destroy the  $\sigma$ -hole by increasing the electron density on Cl and enhance the electron-pair donating ability of Cl for the formation of P...Cl pnictogen bonds.

**Binding Energies.** When Y is the most electronegative substituent F, only one equilibrium H<sub>2</sub>FP:ClF complex is found on the potential surface. It is stabilized by a chlorine-shared halogen bond, with a binding energy of  $-71.1 \text{ kJ mol}^{-1}$ . As the electronegativity of Y decreases in going from F to NC, two H<sub>2</sub>FP:ClNC halogen-bonded complexes exist on the potential surface, one with an ion-pair bond H<sub>2</sub>FP:Cl<sup>+</sup>NC<sup>−</sup>, and the other with a traditional halogen bond. The ion-pair complex has a binding energy of  $-381.2 \text{ kJ mol}^{-1}$  relative to the ions H<sub>2</sub>FP:Cl<sup>+</sup> and NC<sup>−</sup>, while the value of the binding energy is  $+9.0 \text{ kJ mol}^{-1}$  if the neutral H<sub>2</sub>FP and ClNC molecules are considered as the dissociation products. That ClNC forms an ion-pair complex instead of a complex with a chlorine-shared halogen bond as does ClF may be attributed to the ability of NC<sup>−</sup> to better accommodate a full negative charge. Neither ClF nor ClNC form pnictogen-bonded complexes. However, as the electronegativity of Y is further reduced, both halogen-bonded and pnictogen-bonded complexes are found on the H<sub>2</sub>FP:ClCl surface. The chlorine-shared halogen-bonded complex is more stable than the corresponding complex with a traditional halogen bond, but this is not necessarily always the case. For example, H<sub>2</sub>CIP:ClCl also forms complexes with traditional and chlorine-shared halogen bonds, but that with the traditional halogen bond is more stable by  $3 \text{ kJ mol}^{-1}$ . Both halogen-bonded complexes H<sub>2</sub>FP:ClCl are more stable than the corresponding pnictogen-bonded complexes. Only one

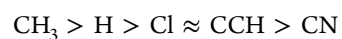
H<sub>2</sub>FP:ClCN halogen-bonded complex with a traditional halogen bond has been found, and its binding energy of  $-8.1 \text{ kJ mol}^{-1}$  is greater than the binding energies of about  $-6.4 \text{ kJ mol}^{-1}$  for the two corresponding pnictogen-bonded complexes. In contrast, both pnictogen-bonded H<sub>2</sub>FP:ClCCH complexes are more stable than the corresponding halogen-bonded complex with a traditional halogen bond. Finally, H<sub>2</sub>FP:ClCH<sub>3</sub> and H<sub>2</sub>FP:ClH form only complexes stabilized by pnictogen bonds. The complex H<sub>2</sub>FP:ClCH<sub>3</sub> ZB-2 has the highest binding energy of  $-18.3 \text{ kJ mol}^{-1}$  among all pnictogen-bonded complexes. Thus, what types of intermolecular bonds are formed and the binding energies of the resulting complexes are determined by the electronegativity of the substituent bonded to Cl. For the halogen-bonded complexes with either chlorine-shared or traditional halogen bonds, the order of decreasing binding energies is



For complexes with pnictogen bonds, the order for ZB-1 complexes is



and for ZB-2 complexes



**Structures.** How are halogen-bonded and pnictogen-bonded complexes distinguished? These complexes can be easily differentiated structurally by the values of the F–P–Cl and P–Cl–A angles, where A is the atom of Y directly bonded to Cl. The data of Table 2 indicate that in halogen-bonded complexes, the Cl atom of CIY is located in approximately one of the tetrahedral directions relative to P, with values of the F–P–Cl angle ranging from  $109$  to  $127^\circ$ , except for values around  $144^\circ$  for the traditional halogen-bonded complex H<sub>2</sub>FP:ClCCH and the chlorine-shared complex H<sub>2</sub>FP:ClCl. At the same time, the P–Cl–A arrangement approaches linearity, with values of this angle greater than  $172^\circ$ , except for the same two complexes H<sub>2</sub>FP:ClCCH and H<sub>2</sub>FP:ClCl. The three types of halogen-bonded complexes are differentiated in terms of their P–Cl and Cl–A distances. Traditional halogen bonds have long P–Cl and short Cl–A distances; chlorine-shared halogen bonds have P–Cl and Cl–A bonds of intermediate lengths; ion-pair bonds have short P–Cl and long Cl–A distances. Thus, from Table 2

it can be seen that the P–Cl distances vary from 3.061 to 3.551 Å in complexes with traditional halogen bonds. The P–Cl distances in the two chlorine-shared halogen-bonded complexes are 2.044 and 2.157 Å, while this distance in the ion-pair complex is 1.970 Å. This distance is similar to the P–Cl distance of 1.930 Å in the cation  $\text{H}_2\text{FPCl}^+$ . The Cl–N distance in the ion-pair complex is 2.246 Å, significantly longer than the distance of 1.624 Å in the ClNC monomer. Cl–A distances in chlorine-shared halogen bonds are longer than the distances in the corresponding monomers, while these distances are similar to the monomer distances when the halogen bonds are traditional.

In contrast to the halogen-bonded complexes, it is the F–P–Cl arrangement which approaches linearity in complexes with pnictogen bonds. The values of this angle are between 162 and 169°, as evident from Table 2. Moreover, the P–Cl–A angles are significantly reduced relative to their values in complexes with halogen bonds. Thus, in ZB-1 complexes the P–Cl–A angle varies between 93 and 110°, while this same angle is reduced to between 81 and 90° in ZB-2. From Table 2 it is also apparent that P–Cl distances do not differentiate between traditional halogen bonds, for which the P–Cl distances vary between 3.061 and 3.551 Å, and pnictogen bonds which have P–Cl distances between 3.121 and 3.437 Å.

**NBO Analyses.** The NBO analyses indicate that charge transfer stabilizes both halogen-bonded and pnictogen-bonded complexes. The charge-transfer energies for these complexes are reported in Table 3. The dominant charge-transfer

**Table 3.**  $\text{P}(\text{lp}) \rightarrow \sigma^*\text{Cl-A}$  and  $\text{Cl}(\text{lp}) \rightarrow \sigma^*\text{P-F}$  Charge-Transfer Energies ( $\text{kJ mol}^{-1}$ ) in Complexes  $\text{H}_2\text{FP:ClY}$  with Halogen Bonds<sup>a</sup> and Pnictogen Bonds

$\text{H}_2\text{FP:ClY}$	XB-T	ZB-1	ZB-2
	$\text{P}(\text{lp}) \rightarrow \sigma^*\text{Cl-A}$	$\text{Cl}(\text{lp}) \rightarrow \sigma^*\text{P-F}$	$\text{Cl}(\text{lp}) \rightarrow \sigma^*\text{P-F}$
Y = NC	17.9		
Cl	23.5	17.7	13.6
CN	4.8	7.4	5.2
CCH	3.5	9.6	7.9
$\text{CH}_3$		19.4	20.4
H		13.6	13.7

<sup>a</sup>The NBO program treats  $\text{H}_2\text{FP:ClF}(\text{XB-S})$ ,  $\text{H}_2\text{FP:ClCl}(\text{XB-S})$ , and  $\text{H}_2\text{FP:ClNC}(\text{XB-IP})$  as ion-pair complexes with very large charge-transfer energies.

interaction in the halogen-bonded complexes XB-T occurs from the lone pair on P of  $\text{H}_2\text{FP}$  to the antibonding  $\sigma^*\text{Cl-A}$

orbital of ClY, as illustrated in Figure 3 for  $\text{H}_2\text{FP:ClCl}$ . These energies vary from 3.5  $\text{kJ mol}^{-1}$  for  $\text{H}_2\text{FP:ClCCH}$  to 23.5  $\text{kJ mol}^{-1}$  for  $\text{H}_2\text{FP:ClCl}$ . In contrast, the dominant charge-transfer interactions in pnictogen-bonded complexes which are also illustrated in Figure 3 occur from the lone pair of Cl to the  $\sigma^*\text{P-F}$  orbital of  $\text{H}_2\text{FP}$ . The charge-transfer energies vary from 7.4 to 19.4  $\text{kJ mol}^{-1}$  for complexes ZB-1 and from 5.2 to 20.4  $\text{kJ mol}^{-1}$  for ZB-2. The weakest charge-transfer interaction in each ZB series occurs in  $\text{H}_2\text{FP:ClCN}$ , and the strongest in  $\text{H}_2\text{FP:ClCH}_3$ . The charge-transfer energies do not correlate with the binding energies of halogen-bonded or pnictogen-bonded complexes but do correlate linearly with the P–Cl distances, with correlation coefficients  $R^2$  of 0.994, 0.950, and 0.941 for the complexes XB-T, ZB-1, and ZB-2, respectively. A plot of the charge-transfer energy versus the P–Cl distance for the ZB-1 complexes is shown in Figure 4.

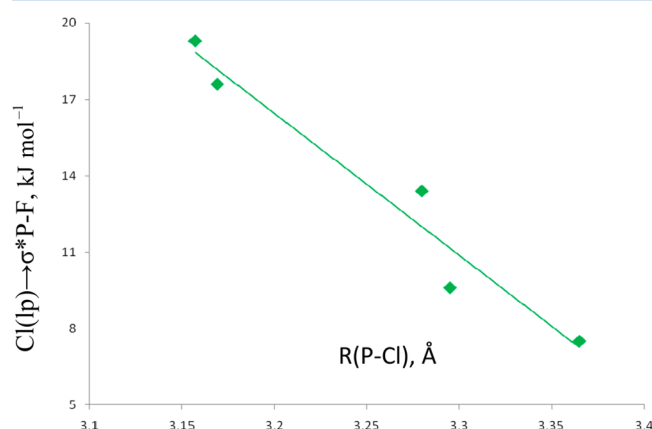


**Figure 4.** Charge-transfer energy  $\text{Cl}(\text{lp}) \rightarrow \sigma^*\text{P-F}$  versus the P–Cl distance for the pnictogen-bonded complexes ZB-1.

The MP2/aug'-cc-pVTZ charges on the  $\text{H}_2\text{FP}$  unit in complexes  $\text{H}_2\text{FP:ClY}$  are listed in Table 4. The NBO charges are consistent with the nature of the charge-transfer interactions in these complexes. In halogen-bonded complexes, the dominant charge-transfer interaction is  $\text{P}(\text{lp}) \rightarrow \sigma^*\text{Cl-A}$ . As a result, the  $\text{H}_2\text{FP}$  unit in these complexes becomes positively charged, with charges ranging from 0.007e in  $\text{H}_2\text{FP:ClCCH}$  to 0.060e in  $\text{H}_2\text{FP:ClCl}$  for complexes with traditional halogen bonds. Of course, the positive charges on the  $\text{H}_2\text{FP}$  units in chlorine-shared and ion-pair complexes are significantly greater, ranging from 0.462e in  $\text{H}_2\text{FP:ClCl}$  to 0.792e in  $\text{H}_2\text{FP:ClNC}$ . In the pnictogen-bonded complexes ZB-

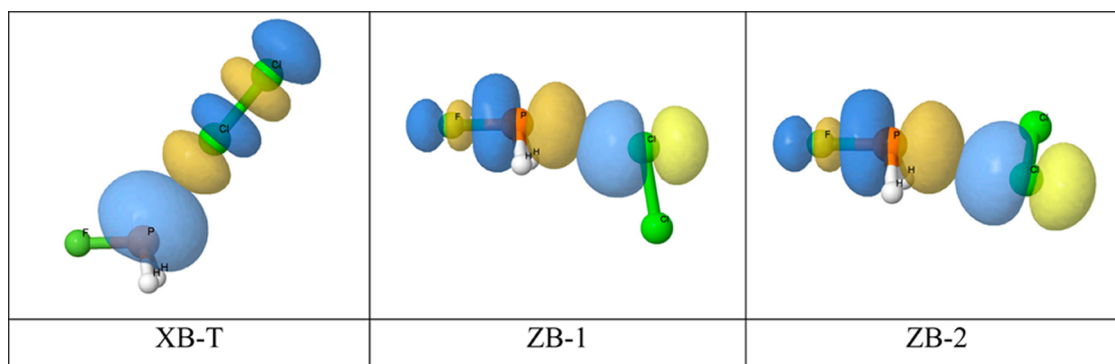


**Figure 3.** Representation of the orbitals involved in the charge-transfer interactions in  $\text{H}_2\text{FP:ClCl}$  complexes XB-T, ZB-1, and ZB-2.



**Table 4.** NBO MP2/aug'-cc-pVTZ Charges on the H<sub>2</sub>FP Unit (au) in Complexes H<sub>2</sub>FP:CIY with Halogen Bonds and Pnicogen Bonds

H <sub>2</sub> FP:CIY	XB-T	XB-S	XB-IP	ZB-1	ZB-2
Y = F		0.654 <sup>a</sup>			
NC	0.038		0.792 <sup>a</sup>		
Cl	0.060	0.462 <sup>a</sup>		-0.016	-0.016
CN	0.011			-0.006	-0.005
CCH	0.007			-0.011	-0.010
CH <sub>3</sub>				-0.023	-0.025
H				-0.014	-0.017

<sup>a</sup>The NBO method treats H<sub>2</sub>FP:ClF(XB-S), H<sub>2</sub>FP:ClCl (XB-S), and H<sub>2</sub>FP:ClNC (XB-IP) as ion-pair complexes.

1 and ZB-2, the dominant charge-transfer interaction is Cl(lp) → σ\*P–F. Thus, the H<sub>2</sub>FP unit in these complexes becomes negatively charged, with the charges varying from -0.005e in H<sub>2</sub>FP:ClCN to -0.025e in H<sub>2</sub>FP:ClCH<sub>3</sub> ZB-2 complexes.

**Electron Densities.** The topological analyses of the electron densities of these complexes show the presence of a P–Cl bond critical point (BCP) and the corresponding bond path connecting the BCP with the P and Cl atoms. These features are illustrated in Table S1 of the Supporting Information. The values of the electron density at the BCP are greater for chlorine-shared and ion-pair halogen bonds, ranging from 0.114 to 0.166 au, and are reduced to between 0.007 and 0.020 au for the weaker interactions in the complexes with traditional halogen bonds and pnicogen bonds. The values of the Laplacian and the total energy density at the BCP are negative for the chlorine-shared and ion-pair halogen bonds, indicating their covalent nature,<sup>34</sup> but are positive for the remaining complexes. A good exponential relationship can be found between the electron density at the P–Cl BCP and the P–Cl distance, in agreement with previous reports.<sup>35–42</sup>

It is interesting to compare the relative positions of the P–Cl BCPs in the complexes with weak traditional halogen bonds and pnicogen bonds. For the traditional halogen bonds, the distance between P and the BCP (d1) is longer than that between Cl and the BCP (d2). The ratio d1/d2 in these complexes is between 1.14 and 1.20. In contrast, in the pnicogen-bonded complexes, d1 is shorter than d2, so that the d1/d2 ratio is between 0.88 and 0.95. These ratios are determined by the atom which acts as the electron-pair donor because the BCP path is longer to that atom because of its higher electron density.

**Coupling Constants.** The one-bond coupling constants <sup>1</sup>XJ(P–Cl) and <sup>1</sup>PJ(P–Cl) and their components for coupling across halogen bonds and pnicogen bonds, respectively, in complexes H<sub>2</sub>FP:CIY are reported in Table S2 of the Supporting Information. These data show that coupling constants for complexes with traditional halogen bonds XB-T, and those with pnicogen bonds ZB-1 and ZB-2, have FC terms which are positive and dominant and good approximations to total J. However, this is not the case for the two complexes XB-S with chlorine-shared halogen bonds. <sup>1</sup>XJ(P–Cl) for H<sub>2</sub>FP:ClCl is dominated by a large positive FC term of 440 Hz, but the PSO term makes a negative contribution of -23 Hz and should not be neglected, although because of the large value of the FC term, neglecting the PSO term introduces an error of only about 4%. H<sub>2</sub>FP:ClF also has a chlorine-shared halogen bond but with a shorter P–Cl distance which is approaching the distance in the cation H<sub>2</sub>FPCl<sup>+</sup>. As a result, the

FC term is significantly reduced but remains positive, and the negative PSO term becomes the dominant term. In this complex, <sup>1</sup>XJ(P–Cl) is reduced to -6 Hz. When the bond becomes an ion-pair bond in H<sub>2</sub>FPCl<sup>+</sup>:NC<sup>-</sup>, the FC term is dominant and negative with a value of -178 Hz, while the PSO term also has a negative value of -41 Hz. The FC term is not a good approximation to total <sup>1</sup>XJ(P–Cl). This pattern is similar to the pattern observed for the cation H<sub>2</sub>FPCl<sup>+</sup>.

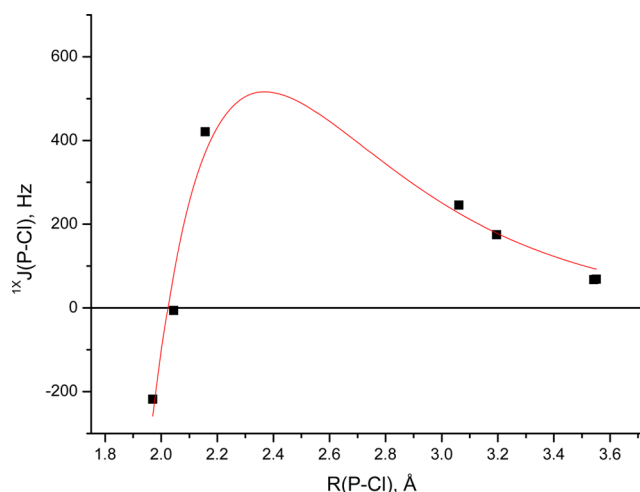
Table 5 provides values of the coupling constant <sup>1</sup>XJ(P–Cl) for the halogen-bonded complexes. As can be seen from these

**Table 5.** Coupling Constants <sup>1</sup>XJ(P–Cl) for Complexes H<sub>2</sub>FP:CIY with Halogen Bonds and <sup>1</sup>PJ(P–Cl) (Hz) for Complexes with Pnicogen Bonds

H <sub>2</sub> FP:CIY	XB-T	XB-S	XB-IP	ZB-1	ZB-2
Y = F		-6.3			
NC	174.8		-217.8 <sup>a</sup>		
Cl	245.4	421.0		56.8	20.2
CN	68.5			24.7	15.6
CCH	67.5			26.8	18.5
CH <sub>3</sub>				40.6	29.0
H				36.8	22.4

<sup>a</sup><sup>1</sup>J(P–Cl) for H<sub>2</sub>FPCl<sup>+</sup> is -153.4 Hz.

data and from the discussion above, the values of this coupling constant span a large range, from -218 Hz in the ion-pair complex to +245 Hz in the H<sub>2</sub>FP:ClCl complex with a traditional halogen bond. How can this behavior be understood? The dependence of <sup>1</sup>XJ(P–Cl) on the P–Cl distance and the nature of the halogen bond is illustrated in Figure 5

**Figure 5.** Coupling constant <sup>1</sup>XJ(P–Cl) versus the P–Cl distance for complexes with halogen bonds.

using a Morse curve. At long distances, <sup>1</sup>XJ(P–Cl) values for complexes with traditional halogen bonds increase as the P–Cl distance decreases. As this distance decreases further, the curvature changes as the halogen bond changes from traditional to chlorine-shared, and <sup>1</sup>XJ(P–Cl) attains its maximum values for chlorine-shared halogen bonds. A further decrease in the P–Cl distance leads to a decrease in <sup>1</sup>XJ(P–Cl) and eventually to a change of sign as the halogen bond changes from chlorine-shared to ion-pair.

<sup>1</sup>PJ(P–Cl) values for the pnicogen-bonded complexes are also reported in Table 5. These values range from 25 to 57 Hz

for complexes ZB-1 and from 16 to 29 Hz for ZB-2. Values for complexes ZB-1 are always greater than the corresponding ZB-2 values, although the P–Cl distances in ZB-1 complexes are not always shorter than those in ZB-2. The tendency for  $^1J(\text{P–Cl})$  to increase as the P–Cl distance decreases can be seen for all pnictogen-bonded complexes, although the data are definitely scattered. Plotting these data for complexes ZB-1 has a correlation coefficient of only 0.705, but the same plot for the ZB-2 complexes in Figure 6 gives a correlation coefficient  $R^2$  of 0.928.

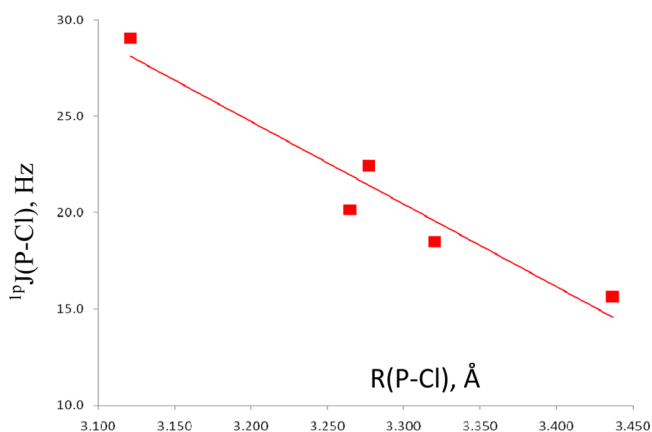


**Figure 6.** Coupling constant  $^1J(\text{P–Cl})$  versus the P–Cl distance for pnictogen-bonded complexes ZB-2.

## CONCLUSIONS

Ab initio MP2/aug'-cc-pVTZ calculations have been carried out on the  $\text{H}_2\text{FP:CIY}$  potential surfaces, for  $\text{Y} = \text{F}, \text{NC}, \text{Cl}, \text{CN}, \text{CCH}, \text{CH}_3$ , and  $\text{H}$ , in search of equilibrium complexes with  $\text{P}\cdots\text{Cl}$  pnictogen bonds and halogen bonds. Three different types of halogen-bonded complexes with traditional, chlorine-shared, and ion-pair halogen bonds and two different pnictogen-bonded complexes have been found on these surfaces.

1. The most electronegative substituents  $\text{F}$  and  $\text{NC}$  form only halogen-bonded complexes, while the most electropositive substituents  $\text{CH}_3$  and  $\text{H}$  form only pnictogen-bonded complexes. The halogen-bonded complexes involving the more electronegative groups  $\text{Cl}$  and  $\text{CN}$  are more stable than the corresponding pnictogen-bonded complexes, while the pnictogen-bonded complexes with  $\text{CCH}$  are more stable than the corresponding halogen-bonded complex. Thus, changing the substituent  $\text{Y}$  of  $\text{CIY}$  can alter the preference for halogen bonds or pnictogen bonds.
2. The substituent  $\text{F}$  forms only one complex with a chlorine-shared halogen bond;  $\text{NC}$  forms complexes with traditional and ion-pair bonds; and  $\text{Cl}$  forms complexes with traditional and chlorine-shared bonds. The substituents  $\text{CN}$  and  $\text{CCH}$  form only complexes with traditional halogen bonds. The substituents  $\text{Cl}$ ,  $\text{CN}$ ,  $\text{CCH}$ ,  $\text{CH}_3$ , and  $\text{H}$  form two types of pnictogen-bonded complexes: one in which the  $\text{P–A}$  bond is *cis* to the bisector of the  $\text{H–P–H}$  angle, and the other in which the  $\text{P–A}$  bond is either *trans* or *gauche* to the bisector.  $\text{A}$  is the atom of  $\text{Y}$  that is directly bonded to  $\text{Cl}$ .
3. Traditional halogen-bonded complexes are stabilized by charge transfer from the  $\text{P}$  lone pair to the  $\text{Cl–A } \sigma^*$

orbital. Charge transfer from the  $\text{Cl}$  lone pair to the  $\text{P–F } \sigma^*$  orbital stabilizes pnictogen-bonded complexes. As a result, the  $\text{H}_2\text{FP}$  unit becomes positively charged in halogen-bonded complexes and negatively charged in pnictogen-bonded complexes.

4. Spin–spin coupling constants  $^{1X}J(\text{P–Cl})$  for complexes with traditional halogen bonds increase with decreasing P–Cl distance, reach a maximum value for complexes with chlorine-shared halogen bonds, and then decrease and change sign for complexes with ion-pair bonds.  $^{1P}J(\text{P–Cl})$  values for coupling across pnictogen bonds tend to increase with decreasing P–Cl distance.

## ASSOCIATED CONTENT

### Supporting Information

Geometries, molecular graphs, and total energies of  $\text{H}_2\text{FP:CIY}$  complexes; components of  $^{1X}J(\text{P–Cl})$  and  $^{1P}J(\text{P–Cl})$  for complexes with halogen bonds and pnictogen bonds, respectively, and  $^1J(\text{P–Cl})$  for  $\text{H}_2\text{FP:Cl}^+$ ; full refs 20 and 33. This material is available free of charge via the Internet at <http://pubs.acs.org>.

## AUTHOR INFORMATION

### Corresponding Authors

\* J.E.D.B.: phone, +330-609-5593; e-mail, [jedelbene@ysu.edu](mailto:jedelbene@ysu.edu).

\* I.A.: phone, +34 915622900; e-mail, [ibon@iqm.csic.es](mailto:ibon@iqm.csic.es).

### Notes

The authors declare no competing financial interest.

## ACKNOWLEDGMENTS

This work was carried out with financial support from the Ministerio de Economía y Competitividad (Project CTQ2012-35513-C02-02) and Comunidad Autónoma de Madrid (Project MADRISOLAR2, ref S2009/PPQ1533). Thanks are also given to the Ohio Supercomputer Center and CTI (CSIC) for their continued support.

## REFERENCES

- (1) Legon, A. C. Prereactive Complexes of Dihalogenes  $\text{XY}$  with Lewis Bases  $\text{B}$  in the Gas Phase: A Systematic Case for the Halogen Analogue  $\text{B}\cdots\text{XY}$  of the Hydrogen Bond  $\text{B}\cdots\text{HX}$ . *Angew. Chem., Int. Ed.* **1999**, *38*, 2686–2714.
- (2) Metrangola, P.; Resnati, G. *Halogen Bonding: Structure and Bonding* 126 Mingos, D. M. P., Ed.; Springer-Verlag: Berlin, 2008.
- (3) Legon, A. C. The Halogen Bond: An Interim Perspective. *Phys. Chem. Chem. Phys.* **2010**, *12*, 7736–7747.
- (4) Zahn, S.; Frank, R.; Hey-Hawkins, E.; Kirchner, B. Pnictogen Bonds: A New Molecular Linker? *Chem.—Eur. J.* **2011**, *17*, 6034–6038.
- (5) Scheiner, S. A New Noncovalent Force: Comparison of  $\text{P}\cdots\text{N}$  Interaction with Hydrogen and Halogen Bonds. *J. Chem. Phys.* **2011**, *134*, 094315.
- (6) Del Bene, J. E.; Alkorta, I.; Sánchez-Sanz, G.; Elguero, J. Structures, Energies, Bonding, and NMR Properties of Pnictogen Complexes  $\text{H}_2\text{XP:NXH}_2$  ( $\text{X} = \text{H}, \text{CH}_3, \text{NH}_2, \text{OH}, \text{F}, \text{Cl}$ ). *J. Phys. Chem. A* **2011**, *115*, 13724–13731.
- (7) Del Bene, J. E.; Alkorta, I.; Sánchez-Sanz, G.; Elguero, J.  $^{31}\text{P}$ – $^{31}\text{P}$  Spin–Spin Coupling Constants for Pnictogen Homodimers. *Chem. Phys. Lett.* **2011**, *512*, 184–187.
- (8) Politzer, P.; Murray, J.; Clark, T. Halogen Bonding and Other  $\sigma$ -Hole Interactions: A Perspective. *Phys. Chem. Chem. Phys.* **2013**, *15*, 11178–11189.
- (9) Bauzá, A.; Alkorta, I.; Frontera, A.; Elguero, J. On the Reliability of Pure and Hybrid DFT Methods for the Evaluation of Halogen,

Chalcogen, and Pnictogen Bonds Involving Anionic and Neutral Electron Donors. *J. Chem. Theory Comput.* **2013**, *9*, 5201–5210.

(10) Scheiner, S. Detailed Comparison of the Pnictogen Bond with Chalcogen, Halogen, and Hydrogen Bonds. *Int. J. Quantum Chem.* **2013**, *113*, 1609–1620.

(11) Scheiner, S. Sensitivity of Noncovalent Bonds to Intermolecular Separation: Hydrogen, Halogen, Chalcogen, and Pnictogen Bonds. *Cryst. Struct. Commun.* **2013**, *15*, 3119–3124.

(12) Solinanejad, M.; Gholipour, A. Revealing Substituent Effects on the Concerted Interaction of Pnictogen, Chalcogen, and Halogen Bonds in Substituted *s*-Triazine Ring. *Struct. Chem.* **2013**, *24*, 1705–1711.

(13) Pople, J. A.; Binkley, J. S.; Seeger, R. Theoretical Models Incorporating Electron Correlation. *Int. J. Quantum Chem., Quantum Chem. Symp.* **1976**, *S10*, 1–19.

(14) Krishnan, R.; Pople, J. A. Approximate Fourth-Order Perturbation Theory of the Electron Correlation Energy. *Int. J. Quantum Chem.* **1978**, *14*, 91–100.

(15) Bartlett, R. J.; Silver, D. M. Many-Body Perturbation Theory Applied to Electron Pair Correlation Energies. I. Closed-Shell First-Row Diatomic Hydrides. *J. Chem. Phys.* **1975**, *62*, 3258–3268.

(16) Bartlett, R. J.; Purvis, G. D. Many-Body Perturbation Theory, Coupled-Pair Many-Electron Theory, and the Importance of Quadruple Excitations for the Correlation Problem. *Int. J. Quantum Chem.* **1978**, *14*, S61–S81.

(17) Del Bene, J. E. Proton Affinities of Ammonia, Water, and Hydrogen Fluoride and their Anions: A Quest for the Basis-Set Limit Using the Dunning Augmented Correlation-Consistent Basis Sets. *J. Phys. Chem.* **1993**, *97*, 107–110.

(18) Dunning, T. H., Jr. Gaussian Basis Sets for Use in Correlated Molecular Calculations. I. The Atoms Boron Through Neon and Hydrogen. *J. Chem. Phys.* **1989**, *90*, 1007–1023.

(19) Woon, D. E.; Dunning, T. H. Gaussian Basis Sets for Use in Correlated Molecular Calculations. V. Core-valence Basis Sets for Boron Through Neon. *J. Chem. Phys.* **1995**, *103*, 4572–4585.

(20) Frisch, M. J.; Trucks, G. W.; Schlegel, H. B.; Scuseria, G. E.; Robb, M. A.; Cheeseman, J. R.; Scalmani, G.; Barone, V.; Mennucci, B.; Petersson, G. A.; et al. *Gaussian 09*, Gaussian, Inc.: Wallingford, CT, 2009.

(21) Bader, R. F. W. A Quantum Theory of Molecular Structure and its Applications. *Chem. Rev.* **1991**, *91*, 893–928.

(22) Bader, R. F. W. *Atoms in Molecules, A Quantum Theory*; Oxford University Press: Oxford, 1990.

(23) Popelier, P. L. A. *Atoms In Molecules. An Introduction*, Prentice Hall: Harlow, England, 2000.

(24) Matta, C. F.; Boyd, R. J. *The Quantum Theory of Atoms in Molecules: From Solid State to DNA and Drug Design*; Wiley-VCH: Weinham, Germany, 2007.

(25) Keith, T. A.; *AIMAll*, version 11.08.23; TK Gristmill Software: Overland Park, KS, 2011; aim.tkgristmill.com.

(26) Reed, A. E.; Curtiss, L. A.; Weinhold, F. Intermolecular Interactions from a Natural Bond Orbital, Donor–Acceptor Viewpoint. *Chem. Rev.* **1988**, *88*, 899–926.

(27) Glendening, E. D.; Badenhoop, J. K.; Reed, A. E.; Carpenter, J. E.; Bohmann, J. A.; Morales, C. M.; Landis, C. R.; Weinhold, F. *NBO 6.0*; University of Wisconsin: Madison, WI, 2013.

(28) Jmol: An Open-source Java Viewer for Chemical Structures in 3D, version 13.0. <http://www.jmol.org/> (accessed September 26, 2013).

(29) Patek, M. “Jmol NBO Visualization Helper” program. <http://www.marcelpatek.com/nbo/nbo.html> (accessed September 26, 2013).

(30) Perera, S. A.; Nooijen, M.; Bartlett, R. J. Electron Correlation Effects on the Theoretical Calculation of Nuclear Magnetic Resonance Spin–Spin Coupling Constants. *J. Chem. Phys.* **1996**, *104*, 3290–3305.

(31) Perera, S. A.; Sekino, H.; Bartlett, R. J. Coupled-Cluster Calculations of Indirect Nuclear Coupling Constants: The Importance of Non-Fermi Contact Contributions. *J. Chem. Phys.* **1994**, *101*, 2186–2191.

(32) Schäfer, A.; Horn, H.; Ahlrichs, R. Fully Optimized Contracted Gaussian Basis Sets for Atoms Li to Kr. *J. Chem. Phys.* **1992**, *97*, 2571–2577.

(33) Stanton, J. F.; Gauss, J.; Watts, J. D.; Nooijen, M.; Oliphant, N.; Perera, S. A.; Szalay, P. G.; Lauderdale, W. J.; Gwaltney, S. R.; Beck, S.; et al. ACES II is a program product of the Quantum Theory Project, University of Florida. Integral packages included are VMOL (J. Almlöf and Taylor PR); VPROPS (P. R. Taylor); ABACUS (T. Helgaker, H. J. Aa. Jensen, P. Jørgensen, J. Olsen, and P. R. Taylor). Brillouin–Wigner perturbation theory was implemented by J. Pittner.

(34) Rozas, I.; Alkorta, I.; Elguero, J. The Behaviour of Ylides Containing N, O and C Atoms as Hydrogen Bond Acceptors. *J. Am. Chem. Soc.* **2000**, *122*, 11154–11161.

(35) Knop, O.; Boyd, R. J.; Choi, S. C. Sulfur–Sulfur Bond Lengths, or Can a Bond length be Estimated from a Single Parameter? *J. Am. Chem. Soc.* **1988**, *110*, 7299–7301.

(36) Alkorta, I.; Barrios, L.; Rozas, I.; Elguero, J. Comparison of Models to Correlate Electron Density at the Bond Critical Point and Bond Distance. *J. Mol. Struct.: THEOCHEM* **2000**, *496*, 131–137.

(37) Knop, O.; Rankin, K. N.; Boyd, R. J. Coming to Grips with N–H···N Bonds. 1. Distance Relationships and Electron Density at the Bond Critical Point. *J. Phys. Chem. A* **2001**, *105*, 6552–6566.

(38) Knop, O.; Rankin, K. N.; Boyd, R. J. Coming to Grips with N–H···N Bonds. 2. Homocorrelations between Parameters Deriving from the Electron Density at the Bond Critical Point. *J. Phys. Chem. A* **2003**, *107*, 272–284.

(39) Espinosa, E.; Alkorta, I.; Elguero, J.; Molins, E. From Weak to Strong Interactions: A Comprehensive Analysis of the Topological and Energetic Properties of the Electron Density Distribution Involving X–H···F–Y Systems. *J. Chem. Phys.* **2002**, *117*, 5529–5542.

(40) Alkorta, I.; Elguero, J. Fluorine–Fluorine Interactions: NMR and AIM Analysis. *Struct. Chem.* **2004**, *15*, 117–120.

(41) Tang, T. H.; Deretey, E.; Knak Jensen, S. J.; Csizmadia, I. G. Hydrogen Bonds: Relation Between Lengths and Electron Densities at Bond Critical Points. *Eur. Phys. J. D* **2006**, *37*, 217–222.

(42) Mata, I.; Alkorta, I.; Molins, E.; Espinosa, E. Universal Features of the Electron Density Distribution in Hydrogen-Bonding Regions: A Comprehensive Study Involving H···X (X = H, C, N, O, F, S, Cl,  $\pi$ ) Interactions. *Chem.—Eur. J.* **2010**, *16*, 2442–2452.